Detailed territorial estimation of design thermal conductivity for façade materials in North-Eastern Spain

José M. Pérez-Bella[a], Javier Domínguez-Hernández[a,*], Enrique Cano-Suñén[a], Mar Alonso-Martínez[b], Juan J. del Coz-Díaz[b]

[a] *Department of Construction Engineering, Engineering and Architecture School, University of Zaragoza, María de Luna, s/n, 50018 Zaragoza, Spain.*

[b] *Department of Construction Engineering, University of Oviedo, Edificio Departamental Viesques nº 7, 33204 Gijón, Spain.*

Abstract

The hygrothermal performance of building envelopes varies based on the temperature and moisture content of their materials. However, multiple building codes adopt constant conductivity values for construction materials based on standardised conditions that do not represent real operating conditions. Currently, a new procedure allows for correcting these normative conductivity values with a limited calculation effort, taking into account the characteristic environmental conditions of each location. This article combines climate records compiled at 313 weather stations distributed in North-Eastern Spain and uses this method to determine the applicable correction factors for materials of masonry façades. The exhaustive characterisation of this geographic area allows for creating correction isopleth maps that may be functionally integrated into building codes to improve the thermal design of buildings at any site of the territory. The results indicate a lower need to correct in mountainous areas, while the Mediterranean coast and the Ebro river valley exhibit larger deviations from normative values with respect to the actual conductivity of the materials. These corrections have been validated in two important cities in this area, Barcelona and Zaragoza.

Keywords

Design thermal conductivity; Building envelope; Isopleth maps; Thermal design; Spain

[*] Corresponding author. Department of Construction Engineering, University of Zaragoza (UZ), María de Luna, s/n, 50018, Zaragoza, Spain. Tel.Fax: +34 976 76 21 00.
E-mail address: javdom@unizar.es (Javier Domínguez-Hernández)

1. Introduction

The design of the thermal envelope of buildings plays a key role in strategies to reduce energy consumption and CO_2 emissions in the construction field [1-4]. The hygrothermal properties of the materials used in the envelope determine the thermal and moisture transfers established between the interior and exterior environments [5-10]. One of the most important properties is thermal conductivity because it defines the thermal transmittance and resistance of enclosures (U-value and R-value, respectively), based on which the requirements of the design used in the majority of building codes are established [11-16].

The thermal conductivity of construction materials varies according to their temperature and moisture content, thus modifying the hygrothermal performance of the entire building [17-19]. Therefore, both climatic parameters should be considered for an appropriate thermal design of the building. Ignoring the characteristic climatic conditions of each location can lead to an incorrect selection of construction materials and enclosure design, greater energy consumption, and a lower hygrothermal performance than expected by design [20-22].

However, several building codes establish constant conductivity values, common for all locations and associated with standardised temperature and humidity conditions in the materials, which do not represent the actual operating conditions of the building enclosures [12-14, 23, 24]. As a result, these standardised conductivity values introduce an additional uncertainty factor in the thermal calculation [25, 26]. In practice, this simplification is preferred over other less functional procedures that would allow for adjusting the conductivity values of each material (e.g., software that requires exhaustive input data or laborious analytical calculations, such as those gathered in standard ISO 10456:2007) [27-30].

However, currently a new procedure allows for adjusting conductivity values in a functional manner, using the input data that are typically available [31]. To achieve this goal, the procedure defines for each location a single factor that is able to correct the standardised conductivity values established in building

codes. To calculate this conductivity correction factor (CCF), the characteristic environmental conditions of each location are considered, which allows for approximating the design thermal conductivity value of the materials for those operating conditions.

Previous studies have determined CCF values that are applicable to materials of common masonry façades in a discrete number of locations distributed across Spain (1 location per 9705 km^2) [31]. However, the different climactic conditions in each site result in correction factors that are not representative in zones far from the locations where they were obtained. Therefore, characterising the entire territory with greater detail constitutes a key factor for developing this procedure, which would allow for adjusting the conductivity values and improving the thermal design of any building, independent of its location.

This article develops this new procedure, providing a detailed characterisation of the CCF values that are applicable to materials of masonry façades in an extensive geographical area. Analysis of the climate data gathered from 313 weather stations in North-Eastern Spain provides exhaustive territorial coverage, reducing the distance between the analysed locations and allowing for a more reliable interpolation of the CCF values obtained. The production of isopleth maps based on these interpolations for two regions of the area (Aragón, 1 station per 568 km^2, and Catalonia, 1 station per 151 km^2) makes it possible to improve the thermal design of any building in both regions, even in locations without representative climate data.

The CCF values obtained have been validated for different masonry façade configurations in the main cities of both regions (Barcelona and Zaragoza). To that end the thermal resistance calculated from standardised conductivity values corrected by CCF values has been compared with the results that would be obtained based on the conductivity values adjusted through the standard ISO 10456:2007.

2. Background

The thermal conductivity of construction materials varies with the temperature and humidity of their porous structures. The range of variations depends on the magnitude of environmental changes and on the intrinsic properties of the material [15, 25, 32-36]. Therefore, each material exhibits a different hygrothermal behaviour considering the variations in its operating conditions.

The thermal conductivity of a material in the operating conditions of the building envelope is described as the design conductivity value, λ_{design} (W/(mK)). These design values should be used for the thermal calculation of the building, thereby characterising its hygrothermal behaviour realistically in each situation [11-14].

However, determining these λ_{design} values is a complex task. The exterior and interior environmental conditions vary over time, according to the climatology of the location and the activity in the building. Similarly, the temperature and humidity of each material varies in every possible configuration of the enclosure, depending on its thickness and the position of the material within the enclosure. In turn, the humidity of materials is not proportional to the relative humidity: the humidity transport mechanisms (i.e., mainly vapour diffusion, capillary flow, capillary condensation, and surface diffusion) are combined differently in each porous structure, leading to a specific sorption function for each material [7, 33, 37-40]. Other additional aspects, such as solar radiation, wind pressure, and wind-driven rain, can also affect the λ_{design} value of materials.

Currently, there are hygrothermal software and calculation procedures capable of integrating these aspects, allowing for precise calculations of λ_{design} values based on the declared conductivity values provided by the material manufacturer or the normative conductivity values established by a building code (both based on standardised temperature and relative humidity conditions).

To consider all design related aspects, hygrothermal software packages use exhaustive input data, such as climate records gathered in short time intervals, expected indoor conditions, and detailed characterisations of material properties [28-30]. Due to the usual lack of such data, these software packages are primarily used in research projects focused on specific case studies [41-43].

In turn, the standard ISO 10456:2007 provides an analytical method based on dimensionless conversion factors associated to temperature (F_T), moisture content (F_M), and ageing (F_A). Using this method (Eq. (1)), the conductivity λ_2 (W/(mK)) of a material in specific environmental conditions can be approximated from a known reference conductivity, λ_1 (W/(mK)), based on other environmental conditions.

$$\lambda_2 = \lambda_1 \cdot F_T \cdot F_M \cdot F_A = \lambda_1 \cdot e^{f_t(T_2 - T_1)} \cdot e^{f_\psi(\psi_2 - \psi_1)} \cdot F_A \quad (1)$$

The calculation employs temperature conversion coefficients f_t (K^{-1}) and moisture conversion coefficients f_ψ (m^3/m^3), tabulated in the ISO standard for various construction materials. The temperature difference $T_2 - T_1$ (K) and moisture content difference $\psi_2 - \psi_1$ (m^3/m^3) for the material must also be identified between both environmental conditions. When Eq. (1) is used to approximate the λ_{design} value based on the declared conductivity specified by the material manufacturer, a correction factor F_A equal to 1 can be adopted (these declared values typically take account of ageing) [27].

Regardless, the need to determine the temperature and relative humidity of each material in the enclosure leads to a laborious process that must be repeated for any variation in thickness, materials, or layer order considered in the design. In addition, to determine the ψ value, it is necessary to have moisture sorption isotherms that empirically characterise the relationship between the relative humidity of the material and its moisture content [40].

Due to the considerable calculation effort and the necessary input data, neither the ISO standard nor the hygrothermal software are useful in practical applications. For that reason, building codes establish normative conductivity values for construction materials (λ_{norm}) that are constant and independent of

operating conditions. To determine their value, standardised conditions (T_{norm} and ψ_{norm}) are adopted, usually coinciding with those used by manufacturers to define their declared values [14, 15, 23, 24]. Thus, although this simplification does not provide a realistic characterisation of the hygrothermal performance of materials, it reduces the complexity of the thermal design and makes its calculation faster.

To reconcile both aspects (i.e., functionality and accuracy), a procedure based on Eq. (1) has recently been developed, which allows for obtaining a simplified estimation of the λ_{design} values with a similar accuracy to that achieved by the ISO standard [31]. For this an adjustment factor is determined, which is only associated to the characteristic climate conditions of each location and can correct the λ_{norm} values established by building codes. The correction factor defined (CCF) is applicable to any material typically present in the analysed enclosure typology (independent of the particular design being considered), allowing for easy implementation in the calculation.

2.1 Correction factor to functionally approximate the design thermal conductivity

To determine the CCF value associated with each location, this new procedure uses the formulation of the ISO standard 10456:2007 (see Eq. (1)) and simplifies its calculation by considering a single generalised enclosure that is representative of an entire typology of enclosures (e.g., masonry façades). This generalised enclosure is assumed to consist of a single uniform and generic material, whose intrinsic properties are obtained by weighting the properties of the materials typically present in the enclosure typology being studied. Thus, its properties can be considered approximately representative of those of the materials present in such enclosures.

The formulation of the ISO standard is used to determine the conversion factors that are applicable to estimate the conductivity of this uniform material in operating conditions (λ_{design}) from its conductivity in the standardised conditions fixed by the building codes (λ_{norm}). The CCF value is defined as the product of the conversion factors ($F_{T\ correction}$ and $F_{M\ correction}$) applicable for the generalised material at each location (Eq. (2)).

$$\lambda_{design} = \lambda_{norm} \cdot CCF = \lambda_{norm} \cdot F_{T\ correction} \cdot F_{M\ correction} \quad (2)$$

Given that this CCF value is calculated for the generic material, the same correction factor can be applied to any real material that is commonly present in the enclosure typology being studied (regardless of the configuration and thicknesses in each specific enclosure). Thus, the correction factor only varies according to the characteristic operating conditions of the location (see Fig. 1). However to extrapolate this CCF value to any real material of the enclosure typology being studied, the conversion coefficients f_t and f_ψ that characterise the uniform material must be representative of these actual materials.

Fig. 1 *A)* Generalisation for determining the correction factor; *B)* Application of CCF value for a particular case of the enclosure typology.

To that end, the various f_t values tabulated in the standard ISO 10456:2007 are used to adopt two mean values: one for the insulating materials (0.00475 K^{-1}) and another for masonry materials (0.002 K^{-1}) [27]. Considering the mean contribution of each material family (insulation and masonry) to the thermal resistance (R-value) of a representative sample of enclosures of the typology being studied, both values are weighted to obtain a single representative value $f_{t\ uniform}$ (K^{-1}) [31].

In turn, the design temperature (T_{design}) of the uniform material in its operating conditions is approximated as the mean value between the average annual temperature at the location, T_{ext}, and the interior temperature established by building codes according to the building use, T_{int}. Given that this T_{int} value is fixed by each building code, the value of $F_{T\ correction}$ depends only on the exterior environmental temperature considered for each location (Eq. (3)).

$$F_{T\ correction} = e^{f_{t\ uniform}\left(T_{design} - T_{norm}\right)} = e^{f_{t\ uniform}\left(\frac{T_{ext}+T_{\mathrm{int}}}{2} - T_{norm}\right)} \quad (3)$$

Similarly, the values of f_{ψ} tabulated in the ISO standard for different materials can be used to adopt a mean value for insulating materials (0.0052 m^3/m^3) and for masonry materials (0.0129 m^3/m^3). By using the same weighting procedure applied to calculate $f_{t\ uniform}$, these mean values are also combined to determine a single representative value $f_{\psi\ uniform}$ (m^3/m^3) [31]. Thus, the value of $F_{M\ correction}$ only depends on the moisture content difference of the uniform material between the design conditions and the standardised normative conditions that define λ_{norm} (Eq. (4)).

$$F_{M\ correction} = e^{f_{\psi\ uniform}\left(\psi_{design} - \psi_{norm}\right)} \quad (4)$$

As noted above, the moisture content of each material as a function of its relative humidity is characterised through a specific sorption function. Therefore, to determine the moisture content in the uniform material, one must define a generalised sorption function that is also representative of the functions of the materials that are commonly present in the typology of enclosures being studied.

For this purpose, the procedure adopts in a simplified manner a linear sorption function, considering that the moisture content for a relative humidity of 0% is null [31]. Given that different databases provide the moisture content of various construction materials for a relative humidity of 0.8 (ψ_{80}), one can determine a representative value $\psi_{80\ uniform}$ (m^3/m^3) that characterises this linear sorption function [29].

By using these databases, the mean value of ψ_{80} was established equal to 0.0052 m^3/m^3 for insulating materials, and equal to 0.0129 m^3/m^3 for masonry materials (averages from a representative sample of tabulated values in databases) [31]. Again, both values can be weighted considering the mean contribution of both material families to the R-value of a representation of enclosures of the typology being analysed ($R_{contribution}$). Thus, the resulting value $\psi_{80\ uniform}$ defines the linear sorption function that characterises the uniform material (Eq. (5)).

$$\psi_{\phi\ uniform} \approx \phi_{uniform} \cdot \frac{0.0052 \cdot R_{contribution} + 0.0129 \cdot \left(1 - R_{contribution}\right)}{0.8} \quad (5)$$

The relative humidity of the uniform material $\phi_{uniform}$ (-) used to determine ψ_{design} (see Eq. (4)) can be calculated in the design conditions by using psychrometric relationships, considering the mean temperature and relative humidity in the location and the interior conditions fixed by building codes [44]. In turn, the standardised value of relative humidity necessary to determine ψ_{norm} is typically provided in the building codes according to standardised conditions.

Anyway, this *CCF* value does not consider various climatic parameters such as wind-driven rain, solar radiation or wind exposure, which may also affect the operating conditions of the construction materials. In addition, the precision of this method depends on the simplifications introduced in Eqs. (3), (4) and (5), which are established according to data collected from materials usually present in the enclosure typology being studied. Integrating more detailed analyses of these enclosures and materials could determine more suitable *CCF* values [31].

2.2 Characterisation of design thermal conductivities in Spanish masonry façades

In Spain, the standardised conditions that define the normative thermal conductivity of construction materials are established in the Building Technical Code (SBTC): a constant temperature of 10˚C and a moisture content at equilibrium at 23˚C and relative humidity of 0.5 [11]. These normative conditions are the same across the entire country and coincide with the declared condition "Ib" established in the ISO standard 10456:2007 for construction material manufacturers.

However, these standardised conditions that define the λ_{norm} values are especially inadequate for the climatology of the Iberian Peninsula. The elevated mean temperatures in Spain (e.g., Madrid, 14.3˚C; Barcelona, 15.3˚C; Valencia, 16.8˚C; Seville, 18.0˚C), in conjunction with the interior environmental

conditions established by the SBTC for buildings (20˚C and a relative humidity of 0.55), result in enclosure materials that commonly exhibit temperatures above 10˚C. In turn, mean relative humidities (varying in provincial capitals from 0.56 in Madrid to 0.79 in Lugo) lead to higher moisture content in the materials than what is considered by the SBTC [45]. All these factors contribute to the λ_{norm} values used being lower than the actual λ_{design} values, favouring optimistic designs for the thermal enclosure and differences between the actual hygrothermal performance of the building and the expectation based on its normative design [20, 21, 25, 32].

To the best of the authors' knowledge, only one study has proposed a general correction of the λ_{norm} values used across the entire country [31]. Applying the functional procedure described above, this study analysed the most common enclosure typology in Spain (masonry façades), thereby calculating the correction factors ($CCF_{façades}$) applicable for materials of these types of façades in 52 Spanish cities.

The weighting coefficient that allows for determining representative values of $f_{t\ uniform}$ and $f_{\psi\ uniform}$ and for solving Eq. (5) was obtained by analysing a representative sample of 25 masonry façade configurations commonly used in Spanish buildings ($R_{contribution}$ equal to 0.565) [31]. As a result, Eqs. (6) and (7) show the linear sorption function that represents the moisture storage in the uniform material and the correction factor that is applicable to the materials in these types of façades, respectively.

$$\psi_{\phi\ uniform} \approx \phi_{uniform} \cdot 0.0107 \tag{6}$$

$$\lambda_{design\ Spanish\ facades} \approx \lambda_{norm} \cdot CCF_{facades} = \lambda_{norm} \cdot e^{0.0036\left(\frac{T_{ext}+20}{2}-10\right)} \cdot e^{4.96\left(\psi_{design}-0.0053\right)} \tag{7}$$

Substituting the relative humidity of the uniform material based on normative conditions ($\phi_{uniform}$ equal to 0.5) in Eq. (6), we obtain its normative moisture content (i.e., 0.0053 m^3/m^3). The moisture content of this uniform material for the design conditions ψ_{design} can also be obtained through Eq. (6). To that end, it is necessary to calculate its relative humidity by using psychrometric relationships based on the exterior environmental conditions and the interior conditions established by the SBTC [45].

Using the mean annual data on the exterior temperature and relative humidity in the 52 provincial capitals of Spain, Eqs. (6) and (7) allowed determining the correction factors applicable for each city. Nevertheless, the climatic variety of the country and its mountainous topography contribute to reducing the validity of these corrections in areas that are far from those capitals (see Table 1) [46, 47]. In addition, the results obtained do not provide correction factors that are suitable for the extreme climate conditions that occur throughout the year because only the mean annual data are considered for each location.

Table 1. Terrain coverage of previous studies [31], compared with the detailed characterisation of two North-Eastern Spanish regions.

This study addresses these limitations by characterising the $CCF_{façades}$ values for masonry façade materials at any location of two extensive regions in North-Eastern Spain: Aragón and Catalonia (see Fig. 2). Eqs. (6) and (7) are combined with climate records obtained from different sources, thereby increasing the density of analysed points in the territory when compared to previous studies. To that end, monthly climate records have been considered, gathered from 296 meteorological stations distributed in both regions and 17 additional stations located in neighbouring regions. The significant reduction in distance between the points being studied (see Table 1) minimises the uncertainty associated with interpolation of the results and allows for a detailed characterisation of the entire territory using CCF isopleth maps. In turn, the analysis of monthly data allows for evaluating different environmental conditions throughout the year, identifying extreme values for the correction factors at each location.

All these developments configure a functional tool to determine the λ_{design} value of façade materials for any building in both regions (even those that are far from important urban centres or in locations without

representative climate records) and allows for improving the thermal designs established by the code at any location.

Fig. 2. Location of both analysed regions and the 7 weather stations in these regions considered in previous studies [31]. *Darker colours represent higher altitudes*.

3. Detailed analysis of the North-Eastern Spanish territory

The North-Eastern portion of the Iberian Peninsula exhibits great climatic variety due to the presence of the Mediterranean Sea in the East, the Pyrenees in the North and the Atlantic Ocean in the North-West [47]. Therefore, one can identify Mediterranean climates (on the Catalonian coast), cold desert climates (in South-Eastern Aragón) and even mountain climates in areas of the Pyrenees (with elevations of up to 3404 m in Aragón). Other mountain ranges such as the Iberian System (in Southern and Western Aragón) and the Catalan Coastal System (parallel to the coast) also reach significant heights (2313 and 1707 m, respectively). By contrast, the Ebro river valley in Central Aragón and Southern Catalonia presents elevations below 500 m and a semi-arid climate. In Northern Aragón and Catalonia, the influence of the Atlantic Ocean and the Pyrenees creates an oceanic climate.

The distribution of buildings and urban centres is also unequal in both regions. In Catalonia, the population is concentrated close to the coast (mainly in Barcelona and its surroundings, with more than 3 million inhabitants), with the population density decreasing towards the North-Eastern part of the region. In the interior, only Lleida has a high population (140,000 inhabitants). Regardless, multiple smaller populations are scattered throughout the territory, with up to 63 cities with more than 20,000 inhabitants [48]. In turn, Aragón concentrates more than half of its population in the city of Zaragoza (680,000

inhabitants). Only 3 other urban centres exceed 20,000 inhabitants, with small towns of less than 1000 inhabitants predominating throughout the territory.

To analyse the operating conditions in both regions, climate records that are commonly available (mean monthly values for temperature and relative humidity) have been used. In addition, to achieve a detailed analysis of the entire territory (even locations far away from large urban centres), climate records provided by different sources have been combined. The same analysis can be extrapolated to other regions with similar data.

In Catalonia, the Meteorological Service of Catalonia manages automatic weather stations spread throughout the territory and constitutes the most representative source of data in the region [49]. The altitude of these stations varies between sea level (in several coastal stations) and 2535 m in Boí-Taüll Ski Resort (North-Western Catalonia). Northern Catalonia (Pyrenees) shows a lower density of stations than the coastal and Southern regions.

In turn, Aragón does not have a centralised management of its meteorological data, making it necessary to combine records provided by different public organisations: the Spanish Meteorological Agency (20 stations), the Agroclimatic Information System for Irrigation (34 stations), the Ebro River Basin Authority (16 stations), and the Spanish Directorate-General of Traffic (14 stations) [50-53]. The stations are concentrated in Central and Northern Aragón, while the Southern region (very sparsely populated) has a relatively lower number of stations. Its altitude varies between 125 m in Fraga (Eastern Aragón) and 1650 m close to the international Bielsa-Aragnouet tunnel (on the border with France).

Finally, to interpolate results also in the perimeter areas of both regions, 17 additional stations located in neighbouring regions and distributed around the analysed territory were considered. To that end, additional databases were consulted, which depend on the public agencies of these nearby areas [51, 54, 55].

The age of these climate records varies by source, with most of the data deriving from the last two decades. The most extensive data derive from the Spanish Meteorological Agency (up to 50 years of data), while the most widely used source (the Meteorological Service of Catalonia) shows records up to 16 years old (1997-2012). In some cases, the data series show discontinuities due to maintenance, equipment substitution, or problems related to data management. Regardless, stations with less than two years of records have been excluded because of their low representativeness. In those cases in which daily records were available, averages have been calculated to obtain the corresponding monthly temperature and relative humidity values.

By calculating the mean annual temperature and relative humidity at each location, it becomes possible to solve Eqs. (6) and (7) and thus determine the mean annual value of $CCF_{façades}$. Thus, the mean correction that is applicable to each location for the λ_{norm} values set by the SBTC was established. The mean monthly data used also allow for determining the $CCF_{façades}$ values associated with the climate conditions of each month, thereby evaluating the maximum and minimum corrections that should be applied to the λ_{norm} values throughout the year (see Tables 2 and 3). In order to reduce the number of decimal places, these *CCF* values have been presented as the percentage increase of the normative conductivity values, according to Eq. (8).

$$CCF_{facades\ (\%\ value)} = \left(CCF_{facades} - 1\right) \cdot 100 \tag{8}$$

Table 2. Results obtained in weather stations of Aragón *(for simplicity, only the locations with higher mean correction factors are shown).*

In general, Aragón exhibits mean correction values that vary between +1.75% (Candanchú Ski Resort, with an elevation of 1585 m) and +3.48% (Caspe). The highest values (i.e., there is a greater need to

correct the λ_{norm} values) are concentrated in the Ebro valley and Eastern part of the region, where the persistence of high temperatures is more pronounced. By contrast, the lowest correction factors correspond to mountainous locations in the Pyrenees and the Iberian System.

The maximum monthly corrections are on average 54.8% higher than the annual correction factors, ranging from +5.35% in Caspe to +2.92% in Candanchú. All the maximum values were observed in summer months (July and August) due to the general increase of environmental temperature. The minimum monthly values are on average 44.9% lower than the annual correction, varying between +2.09% in Caspe and +0.94% in the Bielsa-Aragnouet tunnel. Even these minimum values associated with winter months show the need to increase the current λ_{norm} values used by the SBTC for the thermal design of buildings.

Table 3. Results obtained in Catalonian weather stations *(for simplicity, only the locations with higher mean correction factors are shown).*

In general, Catalonia presents higher correction factors than the locations in Aragon (compare Tables 2 and 3). The mean annual correction varies between +4.01% in Deltebre and +1.18% in Espot (2520 m elevation). The highest correction factors correspond to the coast due to the higher temperatures that are characteristic of the Mediterranean climate. Specifically, the locations at the mouth of the Ebro river present especially high corrections. As in Aragón, the lowest values correspond to mountain locations in the Pyrenees.

The maximum monthly values vary between +5.90% in Deltebre to +2.55% in Espot, exceeding by an average of 55.4% the mean annual $CCF_{façades}$ values. These maximum values are almost exclusively associated with the month of August. In turn, the minimum monthly corrections vary between +2.78% in

Amposta (mouth of the Ebro river) and +0.25%, again in Espot. These values are on average 42.9% lower than the annual corrections and, as in Aragón, always define positive correction values that increase thermal conductivity considered by the SBTC for the construction materials.

Together, these findings suggest that the standardised conditions established by the SBTC to define the thermal conductivity of materials (i.e., 10˚C and relative humidity of 0.5) are unsuitable even in the winter months and in high-altitude locations. The $CCF_{façades}$ values proposed are therefore necessary to correct the current λ_{norm} values and estimate more realistic and suitable λ_{design} values for the thermal design of Spanish buildings.

Fig. 3 shows the isopleth map that represents the mean annual $CCF_{façades}$ values at any point in both regions. To develop this map, a linear interpolation of the correction factors obtained at each analysed location was performed. The reduced distance between these points (less than 30 km in all cases) limits the uncertainty inherent to the interpolation and allows for producing smoothed isopleths that are able to characterise the territory in detail. Thus, this map allows for a functional correction of the λ_{norm} values established in Spain for materials of masonry façades by estimating the λ_{design} values at any location and with a reduced calculation effort.

Fig. 3. Isopleth map of the mean annual $CCF_{façades}$ values for materials of masonry façades in North-Eastern Spain (percentage value).

This isopleth map shows the noticeable differences caused by the presence of geographical accidents and the climatic variations in the area. Thus, correction factors are higher on the coast and in the Ebro river valley. These values gradually decrease as the distance from the coast increases. In the North, the presence of the Pyrenees significantly reduces the necessary correction, as also occurs in the mountain

regions of the Catalan Coastal System. In Southern and Western Aragón the correction factors are also lower (due to the lower temperatures and relative humidities of the Iberian System), although this reduction is more progressive.

The variability identified in the Fig. 3 reinforces the need to develop more detailed analyses for the entire territory, by substituting the characterisations based on exhaustive analyses of a reduced number of locations. One can also verify that the correction factors identified in previous studies for the provincial capitals of both regions are consistent with the isopleth distribution obtained in this study [31]. Therefore, although the climate records used in those capitals were more detailed (daily mean records gathered throughout the 1971-2000 period), the results obtained are similar to those shown in Fig. 3, reinforcing the validity of the proposed territorial characterisation.

3.1 Discussion

When analysing the obtained results, it is clearly evident that locations with very different mean annual relative humidity values nevertheless present similar correction factors (see Fig. 4). Therefore, it is not possible to identify a direct correlation between the $CCF_{façades}$ values and one of the two climatic parameters used for their calculation. By contrast, the other climatic parameter (the exterior temperature) has a strong correlation with the correction factor value (see Fig. 5).

Fig. 4. Relationship between the $CCF_{façades}$ values (mean, maximum and minimum) and the mean annual relative humidity for every location (no clear convergence is observed).

These correlations are related to the normative conditions adopted by the SBTC to define the conductivity of construction materials. Thus, the majority of locations present mean annual temperatures that are much higher than 10˚C, further considering that the interior environment of the buildings is maintained at 20˚C. As a result, the enclosure materials are subject to average temperatures much higher than the 10˚C defined by the SBTC. Therefore, a large portion of the correction factor is derived from the conversion factor $F_{T\ correction}$. However, the mean annual relative humidity of the locations (from 0.53 to 0.86) and the mean annual relative humidity established for the interior environment of buildings (0.55) are not significantly different from the normative value (i.e., 0.5). As a result, the conversion factor $F_{M\ correction}$ has a much lower influence on the $CCF_{façades}$ value.

Fig. 5. Best fit-linear relationship between mean $CCF_{façades}$ and exterior temperature, compared to that obtained from previous studies. Maximum and minimum $CCF_{façades}$ values are also shown.

Considering the mean $CCF_{façades}$ values provided by previous studies for the 52 Spanish provincial capitals and the mean annual temperatures of those locations, a linear relationship that is very similar to that in the North-East of the country can also be identified (Fig. 5) [31]. The high coefficient of determination R^2 obtained for both data series suggests that these relationships can be extrapolated to all of Spain, thereby allowing the correction of normative conductivity values even without relative humidity records. This strong convergence can be used to simplify the elaboration of isopleth maps, increasing the number of locations by also including those that only have temperature records. As seen in Fig. 5, similar relationships could be established to characterise the maximum and minimum monthly $CCF_{façades}$ values in each Spanish location.

4. Validation through application cases in Barcelona and Zaragoza

The correction factors obtained have been used to characterise the design R-value of two common masonry façades located in the two most populated cities of North-Eastern Spain, Barcelona and Zaragoza. A similar analysis could also be performed in any other point of the regions being studied. Fig. 6 shows these façades, the intrinsic properties of their materials (including their normative conductivity values), and the environmental conditions considered in each city (from the Barcelona Zoo and Zaragoza Airport weather stations, respectively). Using these λ_{norm} values, both façade configurations reach the minimum limits of thermal resistance established by the SBTC for the climate zones of both cities (i.e., Barcelona 1.333 m^2K/W and Zaragoza 1.667 m^2K/W) [11]. For this calculation, a value of $R_{ext\ air}$ equal to 0.04 m^2K/W for the outside air film and a value of $R_{int\ air}$ equal to 0.13 m^2K/W for the inside air film were considered, in accordance with the SBTC.

Fig. 6. Masonry façade configurations and material properties considered by the SBTC for the R-value calculation.

This same calculation was repeated by adjusting the conductivity values of the materials through the laborious procedure contained in the standard ISO 10456:2007 (i.e., considering the temperature and moisture conversion factors associated with each specific set of environmental conditions in every layer of both façades). The moisture content of each of the materials was obtained through sorption isotherms provided in the databases of the WUFI Light 5.3 software developed by Fraunhofer Institute for Building Physics [29]. As seen in Table 4, the operating conditions in both cities increase the conductivity values considered by the SBTC for the materials, reducing the real thermal resistance of both enclosures.

Table 4. Design R-value calculated using the Spanish Code, the standard ISO 10456:2007, and the proposed correction factor.

In Barcelona, the design R-value of the enclosure varies between 1.295 m^2K/W and 1.323 m^2K/W (August and January, respectively), with a mean annual value of 1.311 m^2K/W. The three R-values are lower than the normative value previously calculated (i.e., 1.353 m^2K/W, see Fig. 6), and none reaches the minimum requirement established by the SBTC for climate zone C. The same situation occurs in Zaragoza, with a mean annual R-value of 1.644 m^2K/W and a monthly variation ranging from 1.634 m^2K/W in August to 1.652 m^2K/W in January. The analysed enclosure also would not reach the requirement imposed for the thermal design of the building in climate zone D (R-value>1.667 m^2K/W). These results confirm the need to functionally adjust the λ_{norm} values that are currently used by the Spanish code.

The detailed territorial map developed (Fig. 3) and the data shown in Tables 2 and 3 provide this functional adjustment: to that end, the λ_{norm} values of each material are multiplied by the correction factor assigned to each location, subsequently calculating the R-value of the enclosure in the usual way (Eq. (9)).

$$R_{value\ corrected} = R_{ext\ air} + \sum \frac{Thickness_i}{CCF_{facades} \cdot \lambda_{norm\ i}} + R_{int\ air} \quad (9)$$

Considering the mean $CCF_{façades}$ value associated with the weather station in the Barcelona Zoo (1.0380), a design R-value for the façade of 1.310 m^2K/W is obtained. Taking as reference the result obtained through the ISO standard, this correction reduces the error of the normative characterisation by more than 95% (see Table 4). In turn, the error is reduced by more than 70% for the enclosure analysed in the city of Zaragoza (design R-value equal to 1.633 m^2K/W), with a mean $CCF_{façaces}$ value of 1.0328 (Zaragoza

airport). In both cases, it is easy to quickly identify the need to increase the R-value of the façades to achieve the requirements established for each climate zone. Similar results can be obtained by adopting correction values extracted from the isopleth map (Fig. 5): for Barcelona, 1.312 m^2K/W (with a $CCF_{façades}$ value of approximately 1.036), and for Zaragoza, 1.632 m^2K/W (with a $CCF_{façades}$ value of approximately 1.033).

The maximum and minimum monthly values of $CCF_{façades}$ can also be used to characterise the hygrothermal behaviour of the enclosure in the environmental conditions of the most extreme months. As seen in Table 4, these extreme values also approximate the value calculated using ISO standard 10456:2007 with reasonable precision, in any case improving the normative characterisation of the SBTC.

Finally, the linear relationship obtained in Fig. 5 can also be used to estimate the mean $CCF_{façades}$ values based only on the exterior temperature. Considering the mean annual temperatures of 17.1˚C in Barcelona and 15.0˚C in Zaragoza, the correction factors that can be calculated (1.0378 for Barcelona and 1.0341 for Zaragoza) would also improve the characterisation of the R-value of both enclosures (1.310 m^2K/W and 1.631 m^2K/W, respectively).

All of these results validate the utility and precision of these correction factors for materials of masonry façades. In turn, the possibility of estimating these corrections based only on temperature data opens the door to more detailed characterisations of the territory, increasing the number of analysed locations and reducing the uncertainty associated with the interpolation of these results. In any case, there are other aspects that can also affect the thermal performance of the façades (e.g., air tightness, intrinsic variability of the thermal conductivity of many construction materials, thermal bridges or convection in the façade air layers), thus minimising the overall effect of the proposed correction value in the thermal calculation. Nevertheless, all these corrections contribute to an effective improvement in the design of the thermal envelope of any building, regardless of the available climate data in its location.

5. Conclusions

This article develops a previous procedure that allows for functionally correcting the standardised values of conductivity established by building codes for construction materials. Considering climate data that are commonly available in any location, these correction factors allow for estimating more suitable thermal conductivity values for the real operating conditions.

By developing this procedure, the bases for a detailed characterisation of the correction factors associated to any point across an extensive geographical area have been presented. Combining different sources of climate data on temperature and relative humidity, the correction factors applicable to materials of masonry façades have been determined in 313 locations of North-Eastern Spain. The high number of points analysed allows for reducing the distance between them and limiting the inherent uncertainty of interpolating the results. Thus, it is possible to produce isopleth maps that can represent the relevant correction even in locations without any available climate data. In addition, the relationships identified in this study suggest that these correction factors can be estimated by only considering temperature records available at each location.

This detailed territorial characterisation can be extended to other regions and countries where the limited number of locations with exhaustive climate data does not allow for a comprehensive characterisation of the design thermal conductivity across the territory. The developed procedure is also applicable to other enclosure typologies, modifying the weighted coefficients that define the equations used.

The analysis performed for the regions of Aragón and Catalonia shows that the standardised conditions used by building codes to define the conductivity of materials can be inadequate for the real operating conditions. The validation of these results by way of two case studies for masonry façades shows that these $CCF_{façades}$ values can contribute to improving the current compliance with building code requirements and defining more appropriate thermal designs for enclosures under their actual operating

conditions. The proposed correction isopleth maps can also be easily implemented in building codes without increasing the complexity of current calculations.

Acknowledgements

This work was partial financed by the Spanish Ministry of Science and Innovation co-financed with FEDER funds under the Research Project BIA2012-31609. We also recognize engineers Alejandro Noguero Lafuente and Alberto Gómez Guerrero for their help in the data collection and processing.

References

[1] N. Aste, A. Angelotti, M. Buzzetti, The influence of the external walls thermal inertia on the energy performance of well insulated buildings, Energy and Buildings 41 (2009) 1181-1187. doi: 10.1016/j.enbuild.2009.06.005

[2] D. Chwieduk, Towards sustainable-energy buildings, Applied Energy 76 (2003) 211-217. doi: 10.1016/S0306-2619(03)00059-X

[3] E. Kossecka, J. Kosny, Influence of insulation configuration on heating and cooling loads in a continuously used building, Energy and Buildings 34/4 (2002) 321–331. doi: 10.1016/S0378-7788(01)00121-9

[4] P.G. Cesaratto, M. de Carli, A measuring campaign of thermal conductance in situ and possible impacts on net energy demand in buildings, Energy and Buildings 59 (2013) 29-36. doi: 10.1016/j.enbuild.2012.08.036

[5] M. Qin, R. Belarbi, A. Aït-Mokhtar, L,O. Nilsson, Coupled heat and moisture transfer in multi-layer building materials, Construction and Building Materials 23 (2009) 967-975. doi: 10.1016/j.conbuildmat.2008.05.015

[6] M. Qin, Whole-building heat, air, and moisture transfer modeling for residential buildings in different climates, HVAC&R Research 17-5 (2011) 860-871. doi: 10.1080/10789669.2011.582918

[7] C. Hall, W.D. Hoff, Water transport in brick, stone and concrete, 2nd. Ed, Spon Press, New York, 2012.

[8] M. Jerman, R. Černý, Effect of moisture content on heat and moisture transport and storage properties of thermal insulation materials, Energy and Buildings 53 (2012) 39-46. doi: 10.1016/j.enbuild.2012.07.002

[9] M. Ordenes, R. Lamberts, S. Güths, Estimation of thermophysical properties using natural signal analysis with heat and moisture transfer model, Energy and Buildings 41 (2009) 1360-1367. doi: 10.1016/j.enbuild.2009.08.008

[10] Y. Zhang, K. Du, J. He, L. Yang, Y. Li, S. Li, Impact factors analysis on the thermal performance of hollow block wall, Energy and Buildings 75 (2014) 330-341. doi: 10.1016/j.enbuild.2014.02.037

[11] Spanish Building Technical Code, Basic document HE 1 Limitation of energy demand, Section 6.1 (in Spanish).

[12] Irish Building Regulations 2011, Technical Guidance Document L - Conservation of fuel and energy - Dwellings, Section 0.3.

[13] National Building Code of Finland, Document C4 Thermal insulation guidelines 2003, Section 4.

[14] Thermal properties of building structures, in CIBSE Guide A - Environmental design, The Chartered Institution of Building Services Engineers, London, 2007.

[15] Heat, air and moisture control in building assemblies, in: SI (Ed.), ASHRAE Handbook of Fundamentals, American Society of Heating, Refrigerating and Air Conditioning Engineers, Atlanta, 2009.

[16] The Building Regulations 2010, Approved Document L1.A - Conservation of fuel and power in new dwellings, Section 4, Government of the United Kingdom, London, 2013.

[17] F. Ochs, W. Heidemann, H. Müller-Steinhagen, Effective thermal conductivity of moistened insulation materials as a function of temperature, International Journal of Heat and Mass Transfer 54 (2008) 539-552. doi: 10.1016/j.ijheatmasstransfer.2007.05.005

[18] J.A. Clarke, P.P. Yaneske, A rational approach to the harmonization of the thermal properties of building materials, Building and Environment 44 (2009) 2046-2055. doi:10.1016/j.buildenv.2009.02.008

[19] M. Dell'Isola, F.R. d'Ambrosio, G. Giovinco, E. Ianniello, Experimental analysis of thermal conductivity for building materials depending on moisture content, International Journal of Thermophysics 33 (2012) 1674-1685. doi: 10.1007/s10765-012-1215-z

[20] F. Domínguez, B. Anderson, J.M. Cejudo, A. Carrillo, Uncertainty in the thermal conductivity of insulation materials, Energy and Buildings 42 (2010) 2159-2168. doi: 10.1019/j.enbuild.2010.07.006

[21] A. Prada, F. Cappelletti, P. Baggio, A. Gasparella, On the effect of material uncertainties in envelope heat transfer simulations, Energy and Buildings 71 (2014) 53-60. doi: 10.1016/j.enbuild.2013.11.083

[22] H.J. Moon, S.H. Ryu, J.T. Kim, The effect of moisture transportation on energy efficiency and IAQ in residential buildings, Energy and Buildings 75 (2014) 439-446. doi: 10.1016/j.enbuild.2014.02.039

[23] DIN 4108-4:2004. Thermal insulation and energy economy in buildings – Hygrothermal design values.

[24] EN 12524:2007. Building materials and products – Hygrothermal properties – Tabulated design values.

[25] A. Abdou, I. Budaiwi, Comparison of thermal conductivity measurements of building insulation materials under various operating temperatures, Journal of Building Physics 29 (2005) 171-184. doi: 10.1177/1744259105056291

[26] I. Budaiwi, A. Abdou, M. Al-Homoud, Variations of thermal conductivity of insulation materials under different operating temperatures: Impact on envelope-induced cooling load, Journal of Architectural Engineering 8/4 (2002) 125–132. doi: 10.1061/(ASCE)1076-0431(2002)8:4(125)

[27] ISO 10456:2007. Building materials and products - Hygrothermal properties - Tabulated design values and procedures for determining declared and design thermal values.

[28] D.M. Burch, J. Chi, 1997. MOIST A PC program for predicting heat and moisture transfer in building envelopes, In: National Institute of Standards and Technology Special Publication 917, Gaithersburg, 1997.

[29] Fraunhofer IBP Software, WUFI light 5.3, http://www.wufi.de/index_e.html (Last accessed 30th January, 2015)

[30] HygIRC 1-D, http://archive.nrc-cnrc.gc.ca/eng/projects/irc/hygirc.html (Last accessed 30th January, 2015)

[31] J.M. Pérez, J. Domínguez, E. Cano, J.J. del Coz, F.P. Álvarez, A correction factor to approximate the design thermal conductivity of building materials: Application to Spanish façades, Energy and Buildings 88 (2015) 153-164. doi: 10.1016/j.enbuild.2014.12.005

[32] P.E. Glaser, I.A. Black, R.S. Lindstrom, F.E. Ruccia, A.E. Wechsler, Thermal insulation systems—A survey. NASA Report SP5027, 1967.

[33] H.M. Künzel, Simultaneous heat and moisture transport in building components, one- and two dimensional calculation using simple parameters, PhD dissertation, Fraunhofer IRB Verlag, Stuttgart, 1995.

[34] F. Ochs, H. Müller-Steinhagen, Temperature and moisture dependence of the thermal conductivity of insulation materials, In: NATO Advanced Study Institute on Thermal Energy Storage for Sustainable Energy Consumption, Izmir, Cesme, 2005.

[35] J.J. del Coz, F.P. Álvarez, P.J. García, J. Domínguez, B. Rodríguez, J.M. Pérez, Hygrothermal properties of lightweight concrete: Experiments and numerical fitting study, Construction and Building Materials 40 (2013) 543-555. doi: 10.1016/j.conbuildmat.2012.11.045

[36] A. Karamanos, S. Hadiarakou, A.M. Papadopoulus, The impact of temperature and moisture on the thermal performance of stone wool, Energy and Buildings 40 (2008) 1402-1411. doi: 10.1016/j.enbuild.2008.01.004

[37] R.L. Rowell, Gas and vapour permeability: Surface flow through porous media. Journal of Colloid and Interface Science 37/1 (1971) 242-246. doi: 10.1016/0021-9797(71)90286-4

[38] M. Krus, Moisture transport and storage coeffients of porous mineral building materials - Theoretical principles and new test methods, Fraunhofer IRB Verlag, Stuttgart, 1996.

[39] C. Franzen, P.W. Mirwald, Moisture content of natural stone: static and dynamic equilibrium with atmospheric humidity, Environmental Geology 46 (2004) 391-401. doi: 10.1007/s00254-004-1040-1

[40] ISO 12571:2013, Hygrothermal performance of building materials and products -- Determination of hygroscopic sorption properties.

[41] M. Ibrahim, E. Wurtz, P.H. Biwole, P. Achard, H. Sallee, Hygrothermal performance of exterior walls covered with aerogel-based insulating rendering, Energy and Buildings 84 (2014) 241-251. doi:10.1016/j.enbuild.2014.07.039

[42] K. Ghazi Wakili, B. Binder, M. Zimmermann, Ch. Tanner, Efficiency verification of a combination of high performance andconventional insulation layers in retrofitting a 130-year old building, Energy and Buildings 82 (2014) 237-242. doi: 10.1016/j.enbuild.2014.06.050

[43] P.C.P. Silva, M. Almeida, L. Bragança, V. Mesquita, Development of prefabricated retrofit module towards nearly zero energy buildings, Energy and Buildings 56 (2013) 15-125. doi: 10.1016/j.enbuild.2012.09.034

[44] ISO 13788:2012, Hygrothermal performance of building components and building elements – Internal surface temperature to avoid critical surface humidity and interstitial condensation – Calculation methods.

[45] Spanish Building Technical Code. Associated document DA DB-HE/2 supporting Basic Document HE 1 – Limitation of energy demand - Verifying of the limitation of surface and interstitial condensation in enclosures (in Spanish).

[46] National Atlas of Spain, Ministry of Public Works and Transport - National Geographic Institute, http://www.ign.es/ane/ane1986-2008/ (Last accessed 30th January, 2015)

[47] M. Kottek, J. Grieser, C. Beck, B. Rudolf, F. Rubel, World Map of the Köppen-Geiger climate classification updated. Meteorologische Zeitschrift 15 (2006) 259-263. doi: 10.1127/0941-2948/2006/0130.

[48] Spanish Statistical Office, Spanish Ministry of Economy and Finance, http://www.ine.es/en/welcome.shtml/ (Last accessed 30th January, 2015)

[49] Meteorological Service of Catalonia, Generalitat of Catalonia, http://www.meteo.cat/ (Last accessed 30th January, 2015)

[50] Spanish Meteorological Agency, Spanish Ministry of Agriculture, Food and Environment, http://www.aemet.es/en/portada/ (Last accessed 30th January, 2015)

[51] Agroclimatic Information System for Irrigation, Spanish Ministry of Agriculture, Food and Environment, http://eportal.magrama.gob.es/websiar/SeleccionParametrosMap.aspx?dst=1/ (Last accessed 30th January, 2015)

[52] Hydrological Ebro Confederation (Ebro River Basin Authority), Spanish Ministry of Agriculture, Food and Environment, http://www.saihebro.com/saihebro/index.php?url=/datos/mapas/tipoestacion:T/ (Last accessed 30th January, 2015)

[53] Spanish Directorate-General of Traffic, Spanish Interior ministry, http://infocar.dgt.es/etraffic/ (Last accessed 30th January, 2015)

[54] Meteorology and climatology of Navarra, Goverment of Navarra, http://meteo.navarra.es/ (Last accessed 30th January, 2015)

[55] Valencian Institute of Agrarian Research, Generalitat Valenciana , http://riegos.ivia.es/ (Last accessed 30th January, 2014)

List of tables

Table 1. Terrain coverage of previous studies [31], compared with the detailed characterisation of two North-Eastern Spanish regions.

Table 2. Results obtained in weather stations of Aragón *(for simplicity, only the locations with higher mean correction factors are shown)*.

Table 3. Results obtained in Catalonian weather stations *(for simplicity, only the locations with higher mean correction factors are shown)*.

Table 4. Design R-value calculated using the Spanish Code, the standard ISO 10456:2007, and the proposed correction factor.

Table 1.
Terrain coverage of previous studies [31], compared with the detailed characterisation of two North-Eastern Spanish regions.

	Spain		Aragón		Catalonia	
	Analysed locations	**Coverage (results/km^2)**	**Analysed locations**	**Coverage (results/km^2)**	**Analysed locations**	**Coverage (results/km^2)**
Previous work	52	1/9705	3 [(1)]	1/15906	4 [(1)]	1/8027
Current study [(2)]	-	-	84	1/568	212	1/151

[(1)] Locations included within the 52 province capitals; [(2)]17 additional stations were analysed in neighboring regions.

Table 2.
Results obtained in weather stations of Aragón *(for simplicity only the locations with higher mean correction factor are shown).*

Location	Latitude (DD)	Longitude (DD)	Altitude (m)	Years considered	Mean annual $CCF_{façades}$ (% value)	Max. monthly $CCF_{façades}$ (% value)	Min. monthly $CCF_{façades}$ (% value)
Caspe (No. 1)	41.1367	0.0023	255	2008-2013	+3.48	+5.35 (Aug.)	+2.09 (Jan.)
Fraga	41.4970	0.3552	125	2004-2013	+3.39	+5.18 (Jul.)	+1.78 (Jan.)
Caspe (north)	41.3058	0.0698	175	2004-2013	+3.37	+5.03 (Jul.)	+1.92 (Dec.)
Quinto de Ebro	41.3902	0.5173	239	2003-2013	+3.34	+4.94 (Aug.)	+1.95 (Jan.)
Zaidín	41.6389	0.2900	175	2003-2013	+3.33	+5.06 (Jul.)	+1.78 (Jan.)
Alcolea de Cinca	41.7428	0.0742	227	2003-2013	+3.32	+5.03 (Jul.)	+1.80 (Jan.)
Osera de Ebro	41.7428	5.9258	253	2005-2013	+3.31	+4.92 (Jul.)	+1.86 (Dec.)
Boquiñeni	41.8456	1.2501	245	2005-2013	+3.28	+4.82 (Jul.)	+1.88 (Dec.)
Zaragoza (Montañana)	41.7151	0.8244	222	2003-2013	+3.28	+4.86 (Jul.)	+1.92 (Dec.)
Zaragoza Airport	41.6716	1.0199	240	1971-2000	+3.28	+4.91 (Aug.)	+1.98 (Jan.)
Fabara	41.1679	0.1541	246	2003-2013	+3.28	+4.94 (Jul.)	+1.88 (Jan.)
Puigmoreno	41.0969	0.2388	315	2003-2013	+3.27	+4.89 (Jul.)	+1.91 (Jan.)
Tamarite de Litera	41.7828	0.3782	221	2003-2013	+3.27	+5.01 (Jul.)	+1.76 (Jan.)
Candasnos	41.4618	0.0954	320	2003-2013	+3.24	+4.94 (Jul.)	+1.83 (Dec.)
Alfántega	41.8238	0.1488	246	2004-2013	+3.24	+4.96 (Jul.)	+1.72 (Jan.)
Belchite	41.3522	0.7203	328	2003-2013	+3.23	+4.80 (Jul.)	+1.90 (Jan.)
Sariñena	41.7732	0.1753	283	2003-2013	+3.22	+4.90 (Jul.)	+1.79 (Jan.)
Highway AP-68 (*km249*)	41.8525	1.3774	210	2003-2013	+3.22	+4.85 (Aug.)	+1.90 (Jan.)
Calanda	40.9611	0.2094	433	2003-2013	+3.21	+4.80 (Jul.)	+1.89 (Feb.)
Híjar	41.2172	0.5280	300	2004-2013	+3.21	+4.83 (Jul.)	+1.82 (Jan.)
El Grado	42.1522	0.2340	454	2008-2013	+3.20	+5.17 (Aug.)	+1.58 (Jan.)
Selgua	41.9415	0.1274	304	2003-2013	+3.20	+4.92 (Jul.)	+1.73 (Feb.)
Castellote	40.7793	0.3171	779	2008-2013	+3.20	+5.00 (Aug.)	+1.82 (Feb.)
Épila	41.5833	1.2821	321	2003-2013	+3.19	+4.74 (Jul.)	+1.89 (Jan.)
Almonacid de la Sierra	41.4539	1.3287	393	2003-2013	+3.18	+4.74 (Jul.)	+1.90 (Feb.)

Table 3.
Results obtained in Catalonian weather stations *(for simplicity, only the locations with higher mean correction factors are shown).*

Location	Latitude (DD)	Longitude (DD)	Altitude (m)	Years considered	Mean annual $CCF_{façades}$ (% value)	Max. monthly $CCF_{façades}$ (% value)	Min. monthly $CCF_{façades}$ (% value)
Deltebre	40.7895	0.7427	2	2001-2008	+4.10	+5.90 (Aug.)	+2.73 (Dec.)
Amposta (No. 1)	40.7086	0.5827	7	1997-2002	+4.05	+5.87 (Aug.)	+2.78 (Jan.)
St. Jaume d'Enveja	40.7090	0.8356	1	2000-2012	+4.03	+5.83 (Aug.)	+2.66 (Jan.)
Badalona (No. 2)	41.4777	2.2529	109	1999-2003	+4.00	+5.69 (Aug.)	+2.67 (Dec.)
Barcelona (Ciutadella)	41.3919	2.1820	8	1997-2001	+3.89	+5.63 (Aug.)	+2.74 (Dec.)
Torredembarra	41.1486	1.4195	2	2000-2012	+3.88	+5.68 (Aug.)	+2.52 (Dec.)
St. Carles de la Ràpita	40.6291	0.6603	0	2001-2012	+3.86	+5.65 (Aug.)	+2.52 (Jan.)
Riba-roja d'Ebre	41.2460	0.4337	69	2001-2011	+3.83	+5.39 (Aug.)	+2.20 (Dec.)
Vilassar de Mar	41.5136	2.3878	44	1999-2012	+3.82	+5.55 (Aug.)	+2.55 (Dec.)
Amposta (No. 2)	40.7096	0.6332	3	2001-2012	+3.82	+5.62 (Aug.)	+2.52 (Jan.)
Barcelona (El Raval)	41.3857	2.1688	33	2007-2012	+3.80	+5.51 (Aug.)	+2.56 (Jan.)
Barcelona (Zoo)	41.3913	2.1896	7	2007-2012	+3.80	+5.53 (Aug.)	+2.51 (Jan.)
Alcanar	40.5597	0.5243	24	2001-2012	+3.80	+5.54 (Aug.)	+2.53 (Jan.)
Lloret de Mar	41.7253	2.8439	63	1997-2002	+3.79	+5.40 (Aug.)	+2.57 (Jan.)
Viladecans	41.3011	2.0390	3	2001-2012	+3.76	+5.54 (Aug.)	+2.41 (Jan.)
Tarragona	41.1058	1.2021	5	2009-2012	+3.75	+5.62 (Aug.)	+2.30 (Feb.)
Cunit	41.2037	1.6345	17	2007-2012	+3.74	+5.52 (Aug.)	+2.43 (Jan.)
La Sénia	40.6349	0.2808	357	1997-2001	+3.74	+5.45 (Aug.)	+2.54 (Jan.)
Botarell	41.1559	0.9988	231	1999-2003	+3.72	+5.41 (Aug.)	+2.39 (Jan.)
El Prat de Llobregat	41.3423	20813	8	2011-2012	+3.72	+5.59 (Aug.)	+1.78 (Feb.)
L'Aldea	40.7713	0.6174	62	2001-2012	+3.70	+5.42 (Aug.)	+2.42 (Jan.)
Badalona (Museum)	41.4540	2.2487	42	2007-2012	+3.70	+5.38 (Aug.)	+2.44 (Jan.)
Cabrils	41.5196	2.3781	81	2001-2012	+3.70	+5.35 (Aug.)	+2.47 (Jan.)
El Vendrell	41.2174	1.5223	59	1999-2012	+3.69	+5.45 (Aug.)	+2.34 (Jan.)
Caldes de Montbui (No.1)	41.6146	2.1703	130	2001-2007	+3.69	+5.46 (Aug.)	+2.22 (Dec.)

Table 4.
Design R-value calculated using the Spanish Code, the standard ISO 10456:2007 and the proposed correction factor.

				Design R-value to be used in thermal calculations (m^2K/W)		
Location	Ambient condition	Temperature (ºC)	Relative humidity (-)	Normative value [11]	ISO 10456:2007 [27]	Corrected value
Barcelona	Mean annual	17.1	0.67	1.353>1.333 (zone C)	1.311	1.310 (1)
	Max. (August)	25.2	0.69		1.295	1.291 (1)
	Min. (January)	10.2	0.68		1.323	1.324 (1)
Zaragoza	Mean annual	15.0	0.63	1.681>1.667 (zone D)	1.644	1.633 (2)
	Max. (August)	24.5	0.53		1.634	1.610 (2)
	Min. (January)	7.1	0.75		1.652	1.651 (2)

(1) $CCF_{façades}$ values of Barcelona Zoo (Table 3); (2) $CCF_{façades}$ values of Zaragoza Airport (Table 2).

Figure captions

Fig. 1 *A)* Generalisation for determining the correction factor; *B)* Application of CCF value for a particular case of the enclosure typology.

Fig. 2. Location of both analysed regions and the 7 weather stations in these regions considered in previous studies [31]. *Darker colours represent higher altitudes.*

Fig. 3. Isopleth map of the mean annual $CCF_{façades}$ values for materials of masonry façades in North-Eastern Spain (percentage value).

Fig. 4. Relationship between the $CCF_{façades}$ values (mean, maximum and minimum) and the mean annual relative humidity for every location (no clear convergence is observed).

Fig. 5. Best fit-linear relationship between mean $CCF_{façades}$ and exterior temperature, compared to that obtained from previous studies. Maximum and minimum $CCF_{façades}$ values are also shown.

Fig. 6. Masonry façade configurations and material properties considered by the SBTC for the R-value calculation.

Figure 1

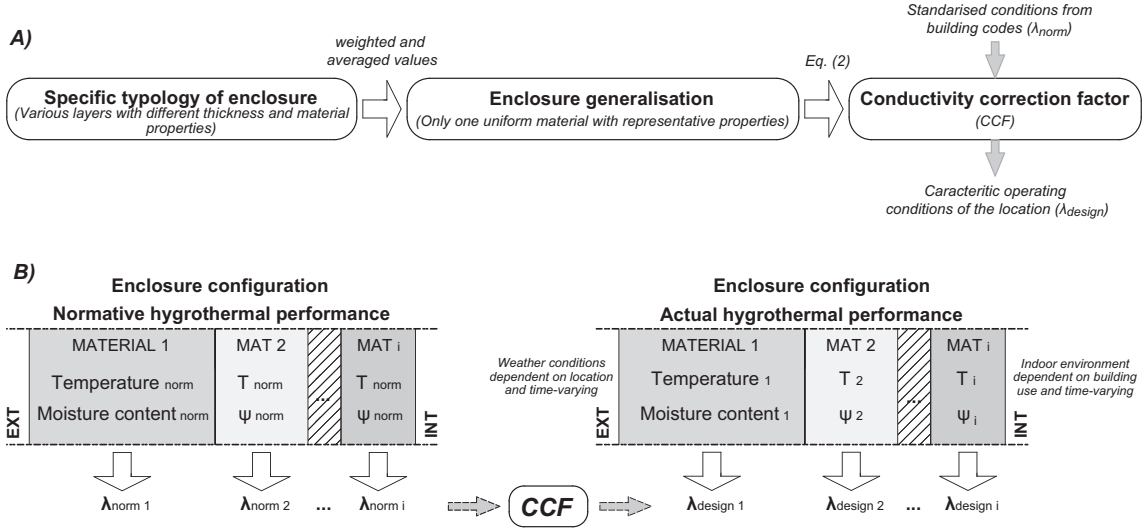

Fig 1. *A)* Generalisation for determining the correction factor; *B)* Application of *CCF* value for a particular case of the enclosure typology.

Figure 2

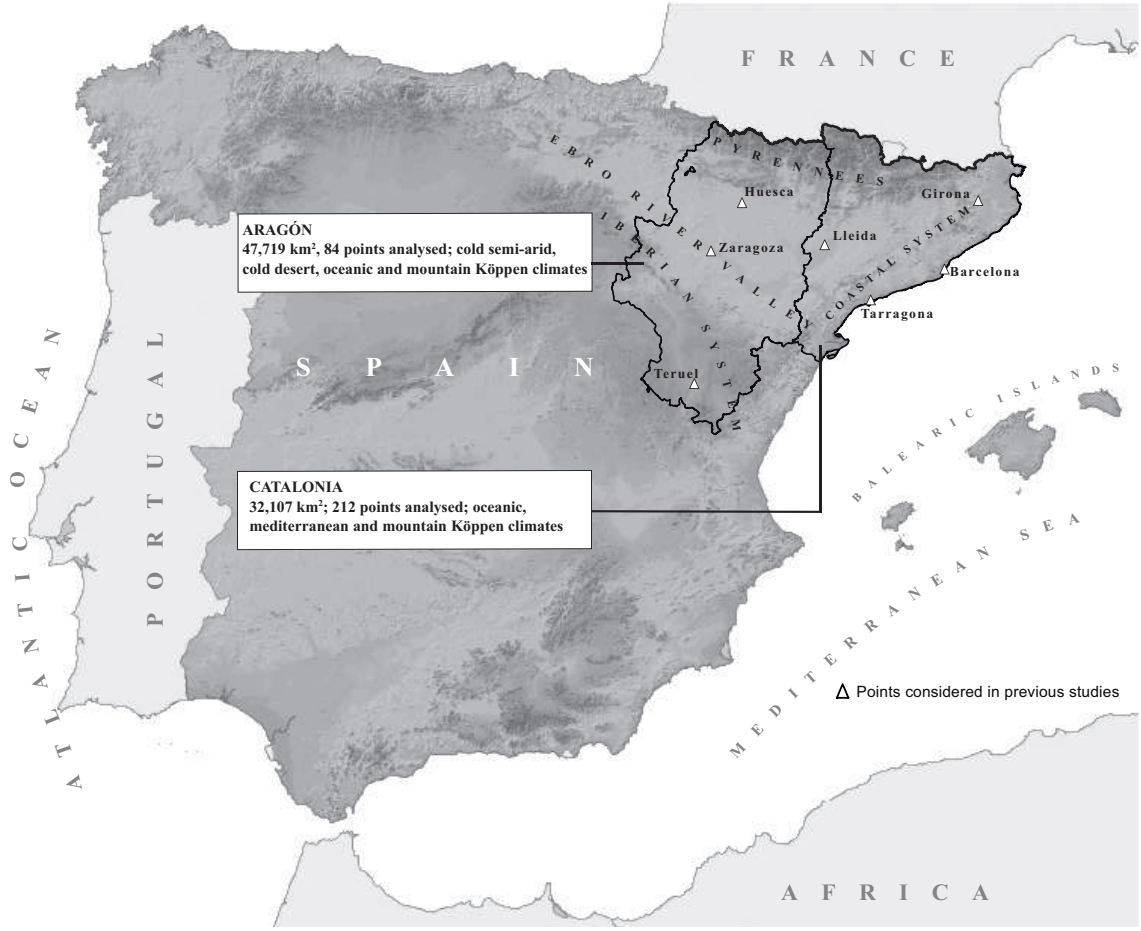

Fig 2. Location of both analysed regions and the 7 weather stations in these regions considered in previous studies [31]. *Darker colours represent higher altitudes.*

Figure 3

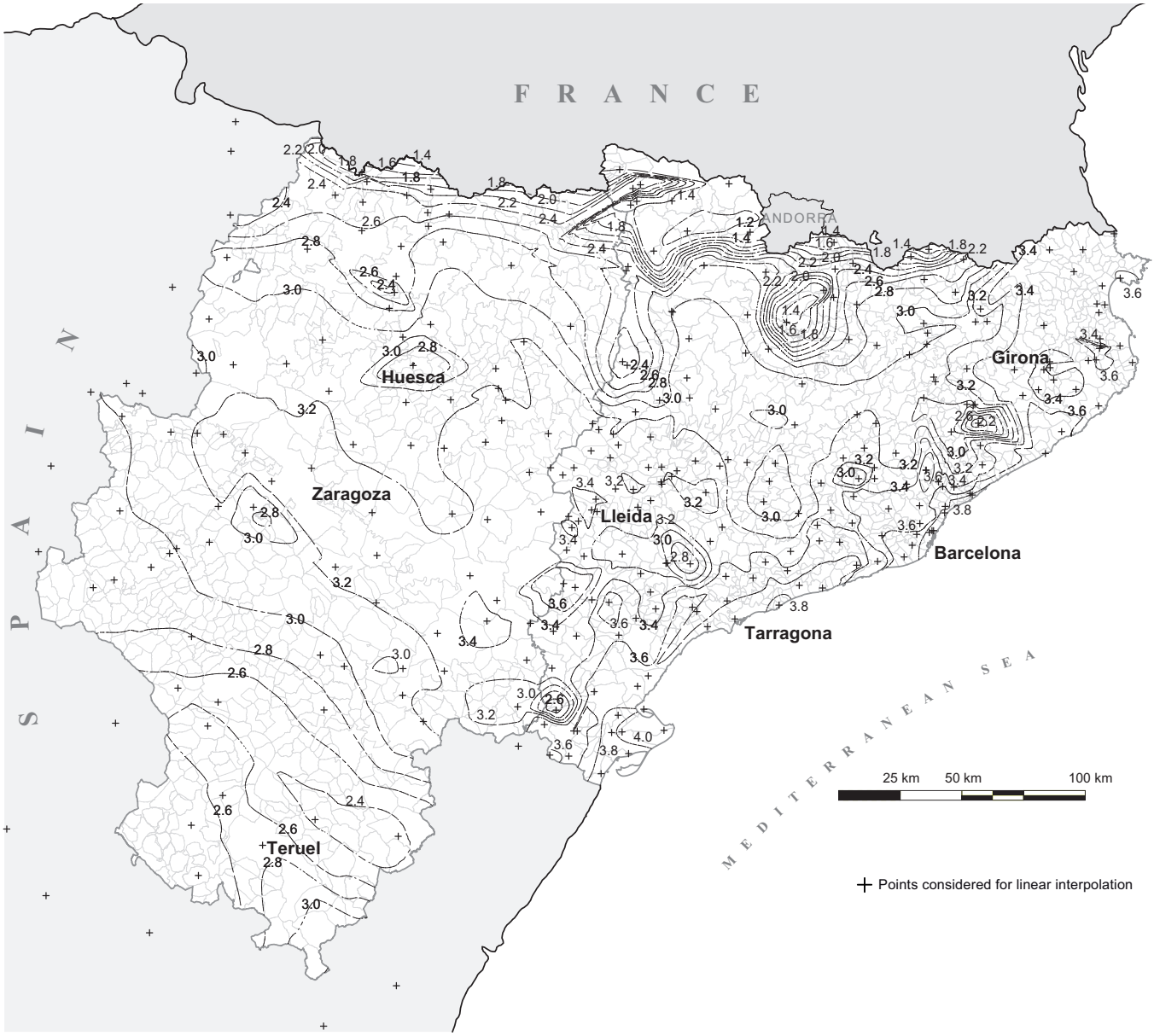

Fig 3. Isopleth map of the mean annual $CCF_{façades}$ values for materials of masonry façades in North-Eastern Spain (percentage value).

Figure 4

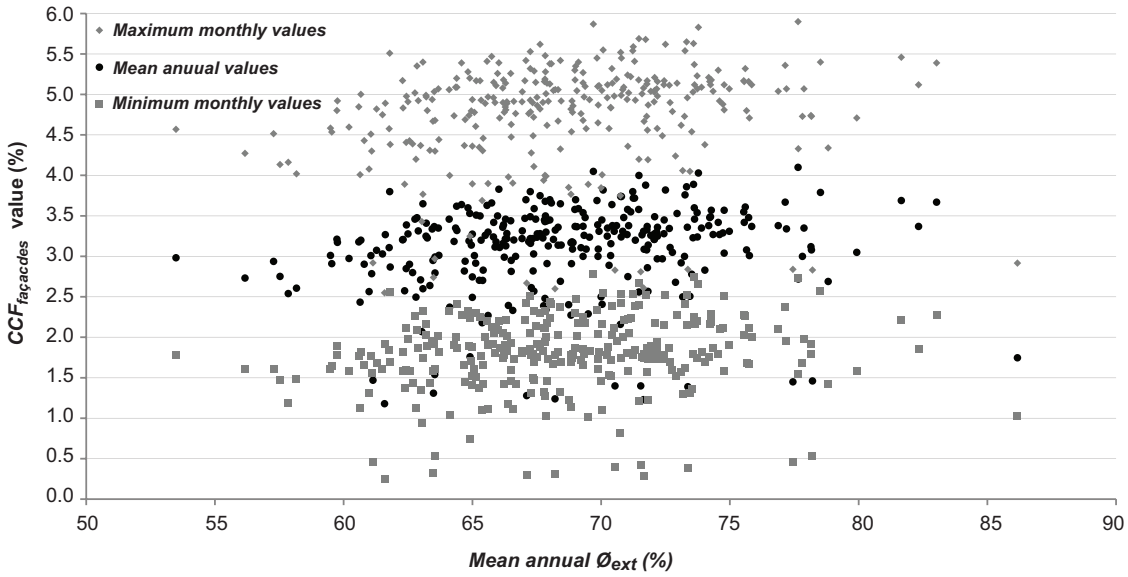

Fig 4. Relationship between the $CCF_{façades}$ values (mean, maximum and minimum) and the mean annual relative humidity for every location (no clear convergence is observed).

Figure 5

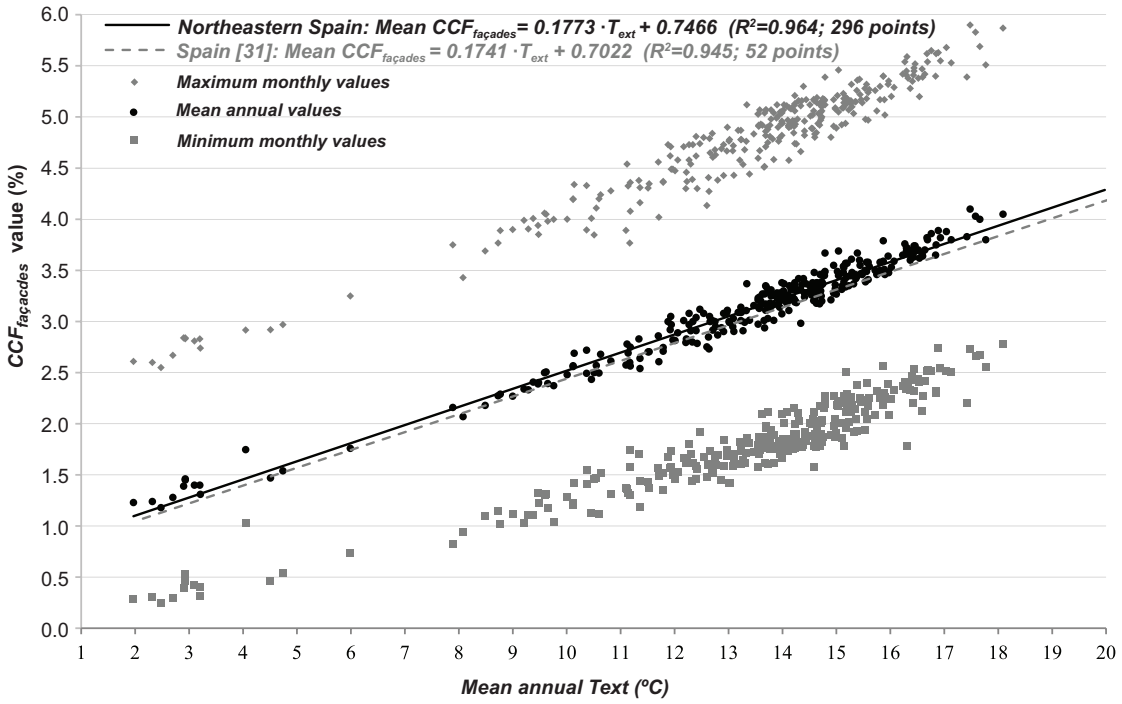

Fig 5. Best fit-linear relationship between mean $CCF_{façades}$ and exterior temperature, compared to that obtained from previous studies. Maximum and minimum $CCF_{façades}$ values are also shown.